Journal of Thermal Analysis and Calorimetry, Vol. 96 (2009) 1, 277–285

SYNTHESIS AND CHARACTERIZATION OF ANTIMONY TRICHLORIDE AND BISMUTH TRICHLORIDE COMPLEXES WITH VALINE

J. G. Shao[1], Y. X. Yang[2], B. W. Li[2], L. P. Zhang[2], Y. R. Chen[2] and X. L. Liu[3]*

[1]College of Chemistry and Chemical Engineering, Yangzhou University, Yangzhou 225002, P.R. China
[2]Department of Chemistry, East China University of Science and Technology, 200237, P.R. China
[3]Analysis Test Center, Yangzhou University, Yangzhou 225009, P.R. China

Two compounds of antimony trichloride and bismuth trichloride with valine are synthesized by solid phase synthesis at room temperature. Their compositions, determined by element analysis, are $Sb(C_5H_{10}O_2N)_3{\cdot}2H_2O$ and $Bi(C_5H_{10}O_2N)_2Cl{\cdot}0.5H_2O$. The crystal structure of antimony complex with valine belongs to triclinic system and its lattice parameters are: a=0.9599 nm, b=1.5068 nm, c=1.9851 nm, α=92.270, β=95.050, γ=104.270. The crystal structure of bismuth complex with valine belongs to monoclinic system and its lattice parameters are: a=1.6012 nm, b=1.8941 nm, c=1.839 nm, β=99.73°. The far-infrared spectra and infrared spectra show that the amino group and carboxyl of valine may be coordinated to antimony and bismuth, respectively, in two compounds. The TG-DSC results also reveal that the complexes were formed.

Keywords: *antimony, bismuth, complexes, solid phase reaction, synthesis, trichloride, valine*

Introduction

The complexes of antimony and bismuth have biological function, such as anti-cancer, sterilization, and so on [1–4]. However, the preparation of the solid complexes of trivalent antimony and bismuth ions is different from that of the other transition metal ions, as the antimony and bismuth ions are easily hydrolyzed in the aqueous solution [5]. The synthesis of the solid complexes of the antimony and bismuth ions by a general solution reaction is very difficult and few complexes of antimony and bismuth are reported. Recently, many transition metal complexes have been obtained by solid phase synthesis [6], but few complexes of antimony and bismuth by solid phase synthesis are reported. In this paper, two complexes of antimony and bismuth with valine are synthesized by solid phase method, and the complexes are characterized by several analytical methods, such as element analysis, X-ray diffraction, far-infrared spectra and TG-DSC.

Experimental

Materials

Reagent

Valine as ligand, lithium hydroxide ($LiOH{\cdot}H_2O$) as alkali to prepare lithium valine salt, antimony trichloride ($SbCl_3$), and bismuth trichoride ($BiCl_3$) can offer positively charged central metal ion Sb^{3+} or Bi^{3+} in following preparation, (the above reagents were all of A.R. grade, Shanghai Chemical Reagent Company Ltd., Shanghai, China).

Synthesis of lithium valine salt

8.7863 g (75 mmol) valine, 40 mL deionized water and 3.147 g (75 mmol) $LiOH{\cdot}H_2O$ were put into the three necked bottle. The mixture was stirred for 4 h at 30°C until the solution was clear. The solvent was rotoray evaporated, filtrated and dried in the vacuum for 1 h. Finally lithium valine salt was obtained.

Synthesis of complex of valine with antimony

1.1075 g (9 mmol) lithium valine and 0.6840 g (3 mmol) antimony trichloride were mixed well together. The mixture was carefully ground in an agate mortar for 30 min and several drops of acetonitrile were added as initiator. At first, the mixture became slightly viscous, indicating that the reaction did happen. Soon after that, the mixture became powdery. One continued grinding for 8 h. The product was dried in the vacuum at 80°C for 4 h and then washed with anhydrous methanol until no chloride ion was found in the washing solution. The obtained powder was next dried in the vacuum at 80°C and finally a new complex of valine with antimony trichloride was obtained.

Synthesis of complex of valine with bismuth

1.1089 g (9 mmol) lithium valine and 0.9395 g (3 mmol) bismuth trichoride were mixed well together. The mix-

* Author for correspondence: yuxyang@online.sh.cn

1388–6150/$20.00

Akadémiai Kiadó, Budapest, Hungary
Springer, Dordrecht, The Netherlands

ture was carefully ground in an agate mortar for 30 min and several drops of acetonitrile were added as initiator. At first, the mixture became slightly viscous, indicating that the reaction did happen. Soon after that, the mixture became powdery. One continued grinding for 8 h. The product was dried in the vacuum at 80°C for 4 h and then washed with anhydrous methanol until no chloride ion was found in the washing solution. The obtained powder was next dried in the vacuum at 80°C and finally a new complex of valine with bismuth trichloride was obtained.

Instrumental methods

Carbon, hydrogen and nitrogen in the complexes were determined by an Elementar Vario EL element analysis. The content of antimony and bismuth in the resultant were measured by TJA IRIS1000 type ICP-AES analysis.

The powder X-ray diffraction patterns of the products, recorded by a Rigaku D/max-2550VB/PC X-ray diffractometer, using CuK_{α_1} radiation, scanning rate 2° (2θ) min^{-1} at room temperature, are presented in Fig. 1. The results of indexing of the X-ray diffraction patterns are listed in Tables 1–3. The far-infrared and infrared spectra of the complexes were measured by a Nicolet 5D-FT spectrometer, using the cesium iodide disk technique. The far-infrared measurements of the standard valine and of the complexes with valine in the range from 50 to 650 cm^{-1} are presented in Figs 2–4, while the infrared spectra of the three complexes in the range from 400 to 4000 cm^{-1} are shown in Fig. 5.

The thermal decomposition process of the resultant was studied by a JETZSCH-STA-449C differential thermal balance in nitrogen using platonic crucibles, with a heating rate of 10°C min^{-1} and α-Al_2O_3 reference. The possible pyrolysis reactions, experimental and calculated percentage mass losses in the thermal decomposition process for the complexes, which resulted from thermogravimetric and differential thermal analysis curves of the complexes are summarized in Tables 4 and 5.

Results and discussions

Element analysis of the compounds

The element analyses indicate that the relative content of the element in complex of antimony valine: C (theor. 35.57%; found 35.03%), H (theor. 6.72%; found 6.56%), N (theor. 8.30%; found 7.99%) and Sb (theor. 24.11%; found 24.74%), respectively. The element analyses yield the composition $Sb(C_5H_{10}O_2N)_3{\cdot}2H_2O$ of the complex. In the molecular formula, a H_2O is considered as adsorbed water. To check whether the new complex contain chloride ions, the synthesized complex was dissolved with concentrated nitric acid. When the $AgNO_3$ was added into the solution, no precipitates were found, which show the new complex does not contain chloride ions, further demonstrate the above molecular formula.

The relative content of the element in complex of bismuth valine: C (theor. 24.72%; found 25.05%), H (theor. 4.33%; found 4.61%), N (theor. 5.77%; found 5.68%) and Bi (theor. 43.00%; found 43.71%), respectively. The element analyses yield the composition $Bi(C_5H_{10}O_2N)_2Cl{\cdot}0.5H_2O$ of the complex. In the molecular formula, 0.5 mol H_2O is considered as adsorbed water. To verify whether the complex of valine with bismuth contain chloride ions, the complex was dissolved by concentrated nitric acid, no sooner the $AgNO_3$ was added into the solution, then the solution began to precipitate, the results show complex contain chloride ions, further demonstrate the above molecular formula.

XRD analysis and discussions of complex for antimony valine, bismuth valine

The X-ray diffraction patterns of the resultants are recorded and shown in Fig. 1. The X-ray diffraction patterns of valine and its complexes all display sharp peak with strong diffraction intensity, and low background. The crystal spacing d_{exp} and relative intensity (I/I_0) of the antimony valine, bismuth valine complexes are completely different from diffraction of ligand valine, and standard diffraction card JCPDS 1-248($SbCl_3$), JCPDS 43-756($BiCl_3$) of the reactants, which demonstrates the reactants have formed new compounds and are not the simple mixtures of metal chlorides with ligand valine.

From the powder X-ray diffraction pattern of the complex bismuth valine shown in Fig. 1, we can also

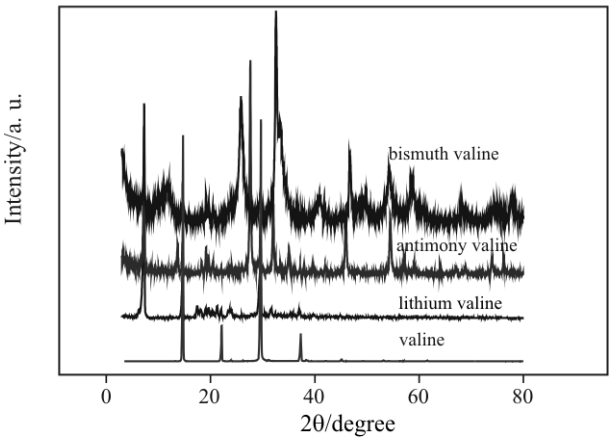

Fig. 1 X-ray patterns of lithium valine, antimony valine and bismuth valine

found that the diffraction peaks are considerably widened, perhaps which reveals the solid complex bismuth valine maybe is nanoparticles. From the widening of the diffraction peaks, we can approximately evaluate the average size of the resultant particles by Scherrer formula. The calculations indicate that the particles of the solid complex are in the nano range and their average size may be less than 100 nm.

The results of indexing to the powder X-ray diffraction pattern are listed in Tables 1–3.

Tables 1–3 show that all the diffraction peaks in the pattern of lithium valine and the complexes antimony valine, bismuth valine can be readily indexed by a set of lattice parameters. The largest relative deviation between the calculated and experimental is less than 0.37%, which indicates that all the three products of the reaction are single phase compounds,

Table 1 The experimental data and the calculated results for powder X-ray diffraction pattern of the lithium valine, monoclinic symmetry: a=1.5024 nm, b=2.0651 nm, c=2.7963 nm, β=100.73°

2θ	D	D_0	$h\,k\,l$	I/%	2θ	D	D_0	$h\,k\,l$	I/%
6.240	14.153	14.1478	1 0–1	3.4	29.560	3.019	3.0199	0 1 9	22.6
7.299	12.101	12.0981	1 0 1	100	30.481	2.93	2.9309	1 5 6	1.5
14.640	6.045	6.049	2 0 2	20.3	31.640	2.825	2.8228	3 0 7	3.4
17.499	5.063	5.067	2 3–1	5.1	32.420	2.759	2.7596	2–6 4	1.0
18.180	4.875	4.8733	1 4 0	2.5	33.380	2.682	2.6828	2 3 8	1.0
19.081	4.647	4.6688	2 3–3	3.4	35.301	2.54	2.5395	1 8–1	1.5
19.620	4.52	4.5121	1 1–6	3.5	36.040	2.49	2.4885	2 6 6	1.0
20.421	4.345	4.331	2 3–4	2.1	37.180	2.416	2.4164	0 8–4	2.6
21.299	4.168	4.1702	2 4–2	4.4	39.860	2.259	2.2594	5–6–1	1.1
22.060	4.026	4.0327	3 2 2	3.2	42.020	2.148	2.1454	2 9 2	0.6
23.999	3.704	3.7117	3 3–4	2.9	44.960	2.014	2.0129	1 8 8	0.4
25.922	3.434	3.4343	0 0 8	0.7	48.720	1.867	1.8668	6 7 1	0.4
27.727	3.214	3.2154	1 0 8	0.3					

Table 2 The experimental data and the calculated results for powder X-ray diffraction pattern of the antimony valine, triclinic symmetry: a=0.9599 nm, b=1.5068 nm, c=1.9851 nm, α=92.27°, β=95.05°, γ=104.27°

2θ	D	D_0	$h\,k\,l$	I/%	2θ	D	D_0	$h\,k\,l$	I/%
7.301	12.096	12.098	0 1–1	61.3	35.984	2.495	2.493	1–4 6	0.7
13.700	6.434	6.458	1 0 2	12.5	37.182	2.419	2.416	0 5–5	2.2
14.641	6.048	6.045	0 2–2	14.1	37.820	2.377	2.376	2 4–4	1.4
18.319	4.829	4.838	1 0 0	5.9	39.539	2.277	2.277	0–5–5	2.0
19.140	4.628	4.633	2–3 0	12.2	39.920	2.258	2.256	0–3 8	1.6
19.641	4.548	4.516	1 0–4	8.0	42.002	2.147	2.149	4–3 3	3.1
20.500	4.320	4.328	1–3 2	5.7	45.078	2.011	2.009	0 7 2	0.6
22.060	4.024	4.026	2–1–3	2.8	45.960	1.975	1.973	4 2 2	31.7
23.720	3.750	3.747	0 1 5	0.9	48.201	1.887	1.886	2 6 2	1.2
24.101	3.688	3.689	1–1–5	3.0	54.480	1.682	1.682	1 7 5	27.8
25.000	3.559	3.558	2 0–4	0.4	57.100	1.609	1.611	1 7 6	7.6
26.001	3.433	3.424	1–3–4	1.8	59.060	1.561	1.562	3 7–1	4.9
27.641	3.218	3.224	1 3–4	100	64.079	1.452	1.452	4 6–5	2.6
28.626	3.114	3.115	3–1–2	1.0	67.000	1.393	1.395	4 6 4	2.9
29.561	3.018	3.019	2 1–5	18.1	68.760	1.366	1.364	2 7 8	2.8
32.021	2.793	2.792	3–1–4	33.6	73.921	1.283	1.281	4 8 0	6.5
32.520	2.753	2.751	3–2 3	5.5	67.220	1.249	1.248	5 5 6	5.6
33.460	2.676	2.675	1–4–5	2.4	77.920	1.225	1.225	4 6 8	1.0
34.981	2.562	2.562	2 0 6	9.2					

Table 3 The experimental data and the calculated results for powder X-ray diffraction pattern of the bismuth valine, monoclinic symmetry: a=1.6012 nm, b=1.8941 nm, c=1.839 nm, β=99.73°

2θ	D	D_0	$h\,k\,l$	I/%	2θ	D	D_0	$h\,k\,l$	I/%
7.280	12.125	12.132	1 1 0	32	37.375	2.404	2.404	–2 0 9	0.4
11.980	7.389	7.381	1 2 1	9.0	40.960	2.203	2.201	0 6 7	9.4
14.640	6.044	6.045	–2 2 1	7	45.021	2.010	2.011	6 4 4	1.2
18.320	4.843	4.838	–2 0 4	5.2	46.760	1.940	1.941	–6 0 9	31.7
19.159	4.625	4.628	0 4 1	11.7	48.480	1.875	1.876	–3 6 9	3.5
19.660	4.500	4.511	–3 1 3	7.9	49.760	1.830	1.830	3 6 8	6.3
20.480	4.334	4.332	0 4 2	4.4	54.260	1.689	1.689	8 0 5	18.4
22.061	4.020	4.025	3 2 2	1.2	58.700	1.571	1.571	5 9 5	15.3
24.100	3.687	3.689	–4 2 1	3.6	60.383	1.530	1.531	8 4 6	1.2
25.900	3.438	3.437	–2 1 6	52.5	68.340	1.371	1.371	9 7 4	7.7
29.599	3.012	3.015	–5 2 2	11.4	69.565	1.351	1.350	8 4 9	1.0
32.600	2.742	2.744	–2 3 7	100.0	74.420	1.274	1.273	7 9 8	4.1
33.440	2.675	2.677	4 3 4	34.5	77.780	1.231	1.226	7 9 9	8.3
63.621	2.452	2.451	–6 2 4	1.7					

the crystal structure of lithium valine belongs to monoclinic system, while the crystal structure of complexes antimony valine and bismuth valine belong to triclinic system and monoclinic system, respectively.

The far infrared spectrum of the compounds

To verify the complex formation between the antimony ion and valine, as well the complex formation between the bismuth ion and valine for further studying coordination properties of complex, we performed far-IR experiments on the complex within the range of spectrum 50–650 cm^{-1}. The far-infrared spectrum of valine, the ligand (lithium salt of valine), the complexes antimony valine and bismuth valine, can be seen from Figs 2–5, respectively.

As shown in Fig. 2, valine shows seven peaks at 542.2, 471.0, 428.6, 376.7, 337.0, 295.9 and 272.7 cm^{-1} in the far-IR region, among which the peak at 542.2 cm^{-1} may be from COO^- vibration, a pair of peaks at 471.0 and 428.6 cm^{-1} may be from NH_3^+ torsion-vibration [7]. Because the free amino acid often exists as an inner salt, there are always both protonated amino group ($–NH_3^+$) and deprotonated carboxyl group ($–COO^-$) in the free amino acid. Besides, a pair of peaks at 376.7 and 337.0 cm^{-1} may be from the $CC^{\alpha}N$ deformation vibration, a pair of peaks at 295.9 and 272.7 cm^{-1} may be from COO^- vibrations [7].

The far-infrared spectrum of lithium valine salt is different from that of valine, as shown in Fig. 3. A new distinct peak at 614.7 cm^{-1} may be from COO^- rocking/wagging/bending vibration [7], which might be coordinated to lithium ion. The spectrum of NH_3^+ torsion-vibration moves to 479.3 and 419.1 cm^{-1}, due

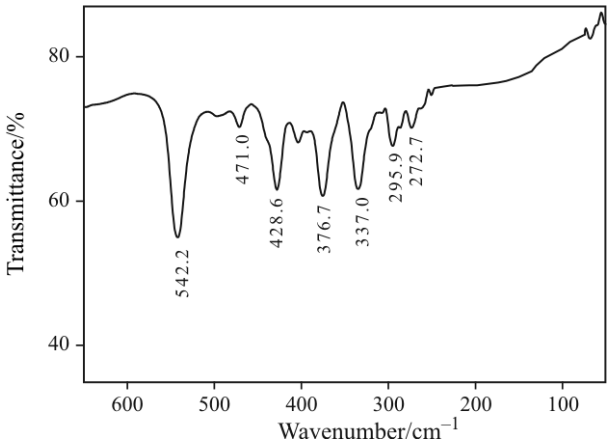

Fig. 2 Far infrared spectrum of standard valine

to there may being only the amino group ($–NH_2$), not any protonated amino group ($–NH_3^+$) in the lithium valine salt. It is also obtained that the spectrum of COO^- vibrations moves to 302.7 and 280.9 cm^{-1} due to coordination between COO^- and lithium ion.

The far infrared spectrums of two complexes antimony valine, bismuth valine are more complicated than the far-infrared spectrum of valine. The difference between Figs 2 and 4 show that the peak at 493.7 cm^{-1} may be from stretching vibration of Sb–N [8] bond, and the peak at 379 cm^{-1} may be from stretching vibration of Sb–O [8] bond, the existence of the Sb–N and Sb–O absorption peaks demonstrate the formation of the complex antimony valine. It is also found that the bands near 542.2 cm^{-1} of the corresponding normal valine shift to 543.1 cm^{-1}, and this phenomenon is also found in far-infrared spectrum of bismuth valine, which verifies the formation of the complex.

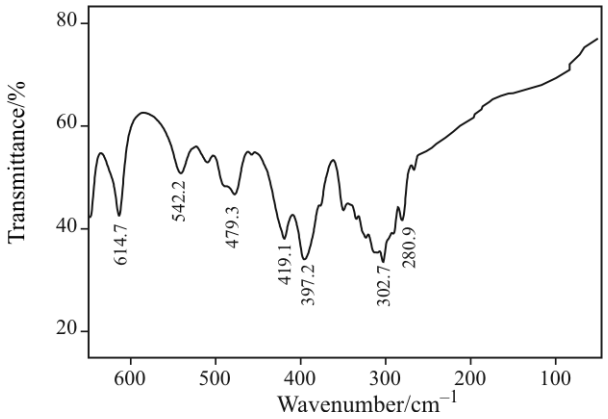

Fig. 3 Far infrared spectrum of lithium valine

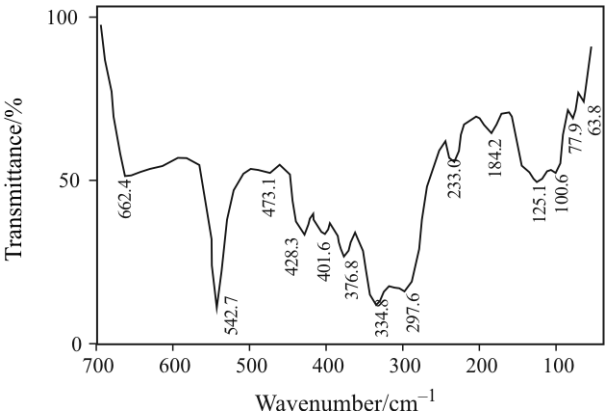

Fig. 5 Far infrared spectrum of bismuth valine

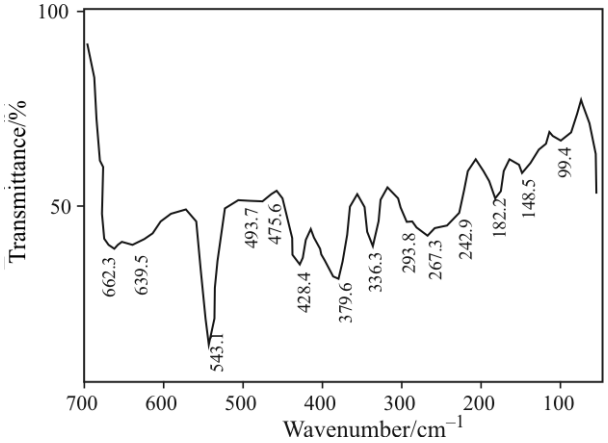

Fig. 4 Far infrared spectrum of antimony valine

In contrast to Fig. 2, the absorption peak at 475 cm^{-1} may be from stretching vibration of Bi–N [8], the absorption peak at 376 cm^{-1} may be from stretching vibration of Bi–O [8] in Fig. 5. While the absorption peak at 77, 63 cm^{-1} can be assigned to symmetry and asymmetric stretching vibration of Bi–Cl bond [9], which indicates the presence of chloride in complex of bismuth valine.

The infrared spectra of compounds

In order to study coordination properties of the complexes, we also performed the IR experiments on the ligand (lithium valine) and the complexes for antimony valine as well as bismuth valine. The following results can be obtained by comparing the standard spectrum of coordination ligand and spectrum of complexes.

As shown in Fig. 6, the IR spectrum of valine displays a distinct peak of hydroxyl group at 3154 cm^{-1}, a distinct peak of H_2O at 1587 cm^{-1}, and three stretching vibrations of C–H bond at 2977, 2947 and 2896 cm^{-1}. Besides, the C–H bond also has two pairs of peaks, 2627 and 1351 cm^{-1} are associated with the stretching or shear deformation vibration of C–H bond in –CH(CH$_3$)$_2$, whereas 2106 and 1329 cm^{-1} are associated with the stretching or shear deformation vibration of C–H bond in –CH–NH$_2$. It is also found that the peaks at 1587 and 1397 cm^{-1} may be due to the symmetric and asymmetric stretching of carboxylic group, and the peak at 1508 cm^{-1} may be due to the stretching vibration of C–O bond. A weak broad peak at 3306 cm^{-1} may be due to stretching vibration of N–H bond. The adsorption peaks at 1329, 1271 and 1034 cm^{-1} may be due to the symmetric and asymmetric stretching or deformation vibration of the N–C bond in the –CH–NH$_2$ group.

For the ligand of lithium valine (Fig. 6), we concluded that the peaks at 2966, 2930 cm^{-1} may be due to the symmetric and asymmetric stretching or deformation vibration of the C–H bond. While the peaks at 3366 and 3285 cm^{-1} can be assigned to symmetry and asymmetric stretching vibration of N–H bond. The adsorption peaks at 1367, 1174 and 1013 cm^{-1} may be due to the symmetric and asymmetric stretching or deformation vibration of the N–C bond in the –CH–NH$_2$ group. The adsorption peaks at 1855, 1581 and 1397 cm^{-1} may be due to the vibrations of carboxylic group.

When the lithium valine was respectively reacted with antimony trichloride and bismuth trichloride to form complexes of antimony valine and bismuth valine, the characteristic peaks of carboxylic group either disappear or shift in the spectrum. For example, the peak at 1581 shift to 1640 cm^{-1}, and the peak at 1855 cm^{-1} disappears, but the peak at 1397 cm^{-1} keeps unchanged. The spectrum of two complexes also shows that the shift in the spectrum of characteristic peaks corresponding to the N–C bond occurs, as can be seen from Fig. 6, the peaks at 1367, 1174 and 1013 cm^{-1}, respectively shift to 1360, 1271 and 1030 cm^{-1}. In the spectrum, the peaks of N–H at 3366 and 3285 cm^{-1} was disappeared. The intensities of the peaks are also changed. Especially, some new peaks were appeared in the spectrum of complex, for example, the peaks corresponding to the C–H bond in –CH(CH$_3$)$_2$ and –CH–NH$_2$ appear at 2631 and 2110 cm^{-1}, respectively. These can be attributed to

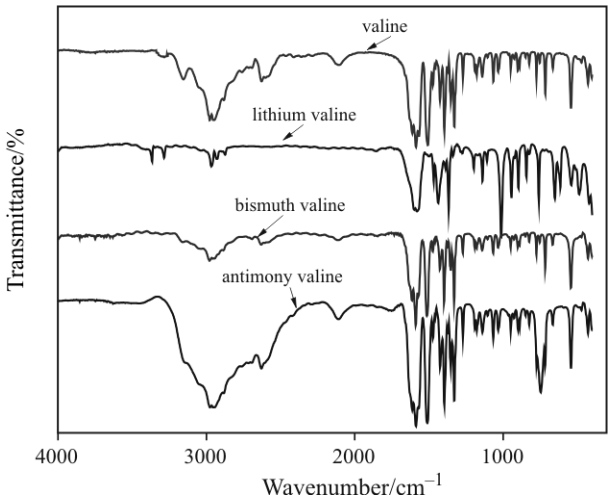

Fig. 6 Infrared spectra of ligand and synthesized complexes

the complex formation between the antimony ion (or bismuth ion) and valine.

It is also found that a very broad adsorption peak at 3400 cm^{-1} appears in the complex of antimony valine, and a comparatively broad adsorption peak at 3400 cm^{-1} appears in the complex of bismuth valine. This demonstrates that the complex of antimony valine contains more amount of H_2O than the complex of bismuth valine.

Thermal decomposition analysis of the compounds

The TG-DSC was made in order to verify the bonds and composition of complex. The results are shown in Figs 7 and 8, the data of possible thermal decomposition processes are shown in Tables 4 and 5, respectively.

Table 4 shows that the first mass loss of the complex $Sb(C_5H_{10}O_2N)_3{\cdot}2H_2O$ begins at about 252°C, the experimental mass loss (25.36%) indicates the losing of $2H_2O$ and $6CH_3$ (the calculated percentage mass loss: 24.92%). The elimination of the H_2O from the complex and cleavage of methyl from isopropyl of valine need certain energy, therefore, there is a considerable endothermic peak at about 252°C in DSC curve.

The second mass loss of the sample occurs at about 270°C and there is a small exothermic peak in DTA curve. It is due to the elimination of 3 moles of $C_2H_2NH_2$, 0.5 mol CO and 0.5 mol CO_2 from the complex. The experimental mass loss (about 31.50%) is close to the calculated one (32.03%). In the thermal decomposition process, the reaction of the pyrolysis products leads to an exothermic peak in DSC curve, probably because the nitrogen atoms of $C_2H_2NH_2$ are not directly coordinated to antimony ion, whereas the loss of CO and CO_2 from the complex indicates carbonyl and CO_2 cleavage from carboxyl directly coordinated to antimony ion, which lead to more stable intermediate compound $(C_2O_4)SbOSb(C_2O_4)$. In that

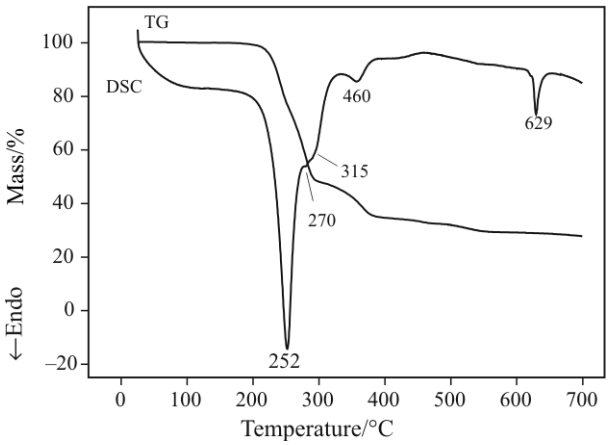

Fig. 7 TG and DSC curves of antimony valine

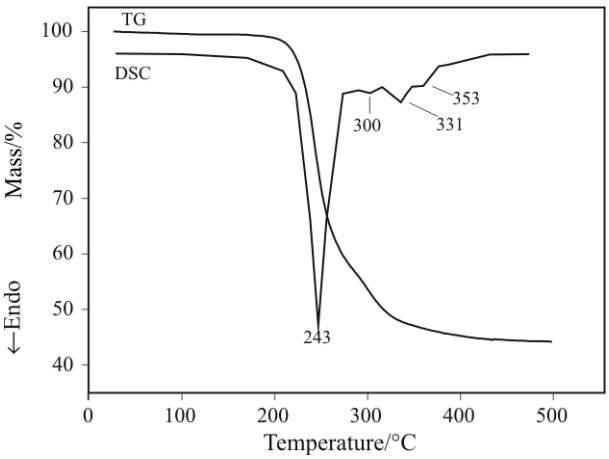

Fig. 8 TG and DSC curves of bismuth valine

case the sample would gradually lose the $C_2H_2NH_2$, CO and CO_2 with increasing temperature.

To check whether the intermediate compound is $(C_2O_4)SbOSb(C_2O_4)$, a certain amount (about 100 mg) of complex $Sb(C_5H_{10}O_2N)_3{\cdot}2H_2O$ was placed in tube type electric-resistance furnace and in nitrogen at 270°C for several minutes, the IR spectrum of cooled sample was observed by a Nicolet 5D-FT spectrometer, as can be seen in the following Fig. 9. It is found that the peak of the symmetric and asymmetric stretching or deformation vibrations of the C–H bond almost disappear, the peaks at 1360, 1271 and 1030 cm^{-1} are also found to disappear, indicating the vibration of the N–C bond in the –CH–NH_2 group has disappeared. The IR spectrum displays peaks of carboxylic group at 1646.1 (strong) and 1530.7 cm^{-1} (medium), whereas a pair of peaks, 735.3 (very strong) and 956.6 cm^{-1} (medium) are associated with the Sb–O–Sb bridge [10], which matches the spectrum of $(C_2O_4)SbOSb(C_2O_4)$. The new strong peak at 3271 cm^{-1} may be due to the antimony oxalate hydrate, because the intermediate compound $(C_2O_4)SbOSb(C_2O_4)$ is easily hydrolyzed by moist air before observation of IR spectrum.

Table 4 Thermal decomposition data of complex $Sb(C_5H_{10}O_2N)_3{\cdot}2H_2O$

Reaction	T/°C	Mass loss/%	
		$M_{exp.}$	$M_{theor.}$
$Sb(C_5H_{10}NO_2)_3{\cdot}2H_2O$			
$\downarrow -2H_2O;\ -2{\cdot}3CH_3;$	252 (endo.)	25.36	24.92
$SbC_9N_3H_{12}O_6$			
$\downarrow -3C_2H_2NH_2;\ 1/2CO;\ 1/2CO_2;$	270 (exo.)	31.50	32.03
$1/2\{(C_2O_4)SbOSb(C_2O_4)\}$			
$\downarrow -2CO$	315 (endo.)	11.14	11.06
$1/2(O_2SbOSbO_2)$			
$\downarrow -1/2O_2;$	460 (endo.)	2.87	3.16
$1/2Sb_2O_3$		29.13	28.80

Table 5 Thermal decomposition data of complex $Bi(C_5H_{10}O_2N)_2Cl{\cdot}0.5H_2O$

Reaction	T/°C	Mass loss/%	
		$M_{exp.}$	$M_{theor.}$
$Bi(C_5H_{10}NO_2)_2Cl{\cdot}0.5H_2O$			
$\downarrow -(CH_3)_2CHNH_2CHCOO;\ -0.5H_2O$	243 (endo.)	26.29	25.76
$0.5[(CH_3)_2CHNH_2CHCOO]Bi(\mu\text{-}Cl_2)Bi[OOCHNH_2CH(CH_3)_2]$			
$\downarrow -(CH_3)_2CHNH_2CHC;\ -0.25O_2$	300 (endo.)	19.00	18.97
$0.5OBiO(\mu\text{-}Cl_2)BiO$			
$\downarrow -0.375Cl_2$	331 (endo.)	5.91	5.47
$0.5OBiO(\mu\text{-}C_{l0.5})BiO^*$			
$\downarrow -0.125Cl_2;$	353 (endo.)	1.46	1.82
$0.5Bi_2O_3$		47.34	47.98

*Its structure can be seen in the following:

O–Bi–O–Bi–O
|
Cl
|
O–Bi–O–Bi–O

When the temperature is higher than 315°C, the sample will lose the residual organic ligands and become Sb_2O_5. While with temperature increasing over 460°C, the pyrolysis product Sb_2O_5 will lose the oxygen in nitrogen and become gradually to stable Sb_2O_3. Finally the pyrolysis residue is yellow Sb_2O_3 powder.

Similarly, the solid complex $Bi(C_5H_{10}O_2N)_2Cl{\cdot}0.5H_2O$ will also lose 0.5 mol water molecule and 1 mole organic ligands $(CH_3)_2CHNH_2CHCOO$, the experimental mass loss (about 26.29%) is close to the calculated one (25.76%). The cleavage of ligands $(CH_3)_2CHNH_2CHCOO$ from the solid complex also need certain energy, therefore, there is a considerable endothermic peak at about 243°C in DSC curve. Then, at 300°C, the sample will cleave $(CH_3)_2CHNH_2CHC$ and $0.25O_2$ from $(CH_3)_2CHNH_2CHCOO$, the elimination of the $(CH_3)_2CHNH_2CHC$ from the complex need certain energy, and thus, there is a corresponding endothermic peak in DSC curve.

To check whether the first intermediate compound is $[(CH_3)_2CHNH_2CHCOO]Bi(\mu\text{-}Cl_2)Bi[OOCHNH_2CH(CH_3)_2]$ and the second intermediate compound is $OBiO(\mu\text{-}Cl_2)BiO$, two certain amounts (about 100 mg) of complex $Bi(C_5H_{10}NO_2)_2Cl{\cdot}0.5H_2O$ were placed in tube type electric-resistance furnace and in nitrogen at 243 and 300°C, respectively for several minutes, the IR spectrum of cooled samples were observed by a Nicolet 5D-FT spectrometer, as can be seen in the following Figs 10a and b.

In Fig. 10a, the IR spectrum appears a strong peak at 471.2 cm^{-1} due to the Bi–Cl–Bi bridge vibration [11], and a medium peak at 1628.7 cm^{-1} due to carboxylic group vibration. At 1103.7 cm^{-1} appears a very strong peak due to the N–C bond in organic ligand $[(CH_3)_2CHNH_2CHCOO]$, while a medium peak around 800.0 cm^{-1} is ascribed to Bi–O–Bi linkage vibration [12, 13]. This shows the IR spectrum re-

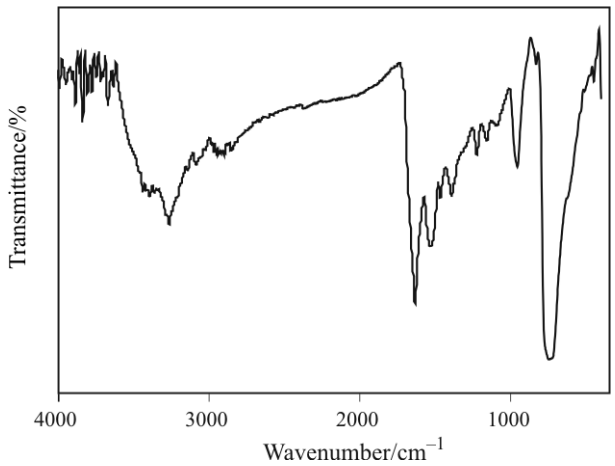

Fig. 9 Infrared spectrum of intermediate compound in Table 4

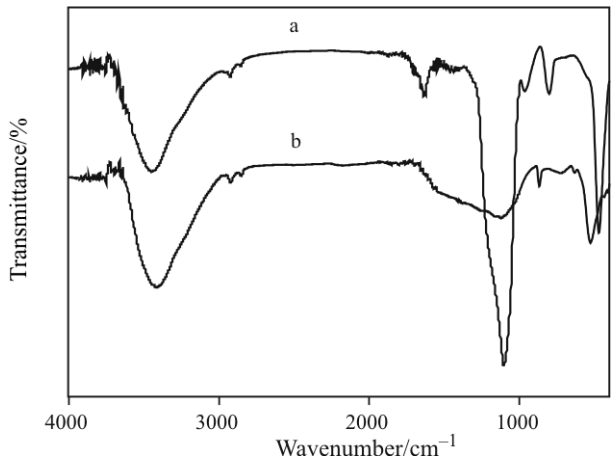

Fig. 10 Infrared spectrum of intermediate compound in Table 5, a – $Bi(C_5H_{10}O_2N)_2Cl{\cdot}0.5H_2O$ complex heated in nitrogen at 243°C, b – $Bi(C_5H_{10}O_2N)_2Cl{\cdot}0.5H_2O$ complex heated in nitrogen at 300°C

corded in Fig. 10a can match the spectrum of $[(CH_3)_2CHNH_2CHCOO]Bi(\mu\text{-}Cl_2)Bi[OOCHNH_2CH(CH_3)_2]$.

When the sample was heated in nitrogen at 300°C, the very strong peak at 1103.7 cm^{-1} sharply decreases, and the peak of carboxylic group at 1628.7 cm^{-1} (medium) is found to be disappeared, indicating the organic ligand $(CH_3)_2CHNH_2CHCOO$ is almost removed from the sample. It is also found that the peak of the Bi–Cl–Bi bridge at 471.2 moves to 528.9 cm^{-1} with peak intensity decreasing, and the peak of the Sb–O at 800.0 cm^{-1} moves to 865.7 cm^{-1}. This shows the IR spectrum recorded in Fig. 10b can match the spectrum of $OBiO(\mu\text{-}Cl_2)BiO$. The results of infrared spectrum further demonstrate the thermal decomposition process of complex $Bi(C_5H_{10}O_2N)_2Cl{\cdot}0.5H_2O$.

Figures 10a and b all show a new strong peak at 3426 cm^{-1}, probably because the intermediate compound is easily hydrolyzed by moist air before observation of IR spectrum.

When temperature is above 331°C, the sample lose the residual chloride ion, forming the products $OBiO(\mu\text{-}Cl_{0.5})BiO$ with the Bi–Cl–Bi bridge, there is also a corresponding endothermic peak in DSC curve. The result is in a good agreement with the far infrared spectrums, further demonstrating the presence of chloride ligand in complex of bismuth valine. When the temperature is higher than 353°C, the sample will lose the residual chloride ions and become Bi_2O_3, the experimental percentage mass loss (47.34%) consists with the calculated that 47.98%. Finally, the residue is yellow Bi_2O_3 powder.

The pyrolysis process of the two samples both shows that the elimination of the nitrogen atoms from complex occurs at one time, indicating there being only one kind of nitrogen atoms in the complex. On the conclusion, it is one nitrogen atom on the amino group of valine that is coordinated directly to antimony ion or bismuth ion, adsorption peaks of Sb–N and Bi–N are determined by far-infrared spectrum, which verify the existence of complex further.

The thermal decomposition process of the two samples also shows that the elimination of the oxygen atoms from complex occurs step by step at two or three different temperatures, but not at one time. Especially, the complex of antimony valine firstly loses CO carbonyl and CO_2, but at last loses $0.5O_2$, indicating the oxygen atom in the complex is coordinated directly to the antimony ion in the complex. In comparison with antimony valine, the complex of bismuth valine firstly loses $(CH_3)_2CHNH_2CHCOO$, secondly loses $0.25O_2$, and at last loses chloride ion, also demonstrating the oxygen atom and chloride atom in the complex are coordinated directly to the bismuth ion in the complex. The adsorption peaks of Sb–O, Bi–O and Bi–Cl determined by far-infrared spectrum certainly verify the existence of complex further.

Conclusions

Two complexes of antimony valine, and bismuth valine can be synthesized by the solid-solid reaction at room temperature. The crystal structure of antimony valine belongs to triclinic system, its lattice parameters are: a=0.9599 nm, b=1.5068 nm, c=1.9851 nm, α=92.270, β=95.050, γ=104.270, while the crystal structure of bismuth valine belongs to monoclinic system, its lattice parameters are: a=1.6012 nm, b=1.8941 nm, c=1.839 nm, β=99.73°. The composition of complex is determined by elemental analysis and ICP-AES analysis, the structure of complex is characterized by XRD, far-infrared, infrared and TG-DSC, which can give the evidence of complex formation between antimony ion (or bismuth ion) and coordination ligand. The results also demon-

strate that the solid complex bismuth valine is nanoparticles, which has not been ever reported by literature before. The amino group and carboxy group of valine are coordinated directly to antimony ion or bismuth ion in the two complexes, the evidence of vibration of Bi–Cl bond in far-infrared spectrum indicates the chloride is bonded directly to bismuth ion.

Acknowledgements

The project was supported by Shanghai Municipal Natural Science Foundation and was supported by the Open Project Program of State Key Laboratory of Inorganic Synthesis and Preparative Chemistry, Jilin University.

References

1 R. Ge and H. Sun, Acc. Chem. Res., 40 (2007) 40 267.
2 Z. Guo-Qing and G. Ying-Chen, Chem. Res. Appl., 14 (2002) 199 (Chinese).
3 G. Cantos, C. L. Barbieri, M. Iacomini, Biochem. J., 289 (1993) 155.
4 X. Xin, J. Solid State Chem., 132 (1997) 291.
5 People's Republic of China Petroleum and Chemical Division Department Standards, HG13-1061-77, Chemical Reagents, Antimony trichloride.
6 G.-Q. Zhong, Appl. Chem. Ind., 31 (2002) 31 (Chinese).
7 Z. Jixin *et al.*, Analytical Chemistry Experiment, East China of Science and Technology, University Press 1989.
8 Y. C. Guo, S. R. Luan, Y. R. Chen, X. S. Zang, Y. Q. Jia and G. Q. Zhong, J. Ther. Anal. Cal., 68 (2002) 1025.
9 A. R. J. Genge, W. Levason and G. Reid, Chem. Commun., (1998) 2159.
10 M. J. Taylor, L.-J. Baker, C. E. F. Rickard and P. W. J. Surman, J. Organomet. Chem., 498 (1995) C14.
11 C. Silvestru and J. E. Drake, Coord. Chem. Rev., 223 (2001) 117.
12 T. J. Boyle, D. M. Pedrotty, B. Scott and J. W. Ziller, Polyhedron, 17 (1998) 1959.
13 P. Pascuta and E. Culea, Mater. Lett., 62 (2008) 4127.

Received: February 1, 2008
Accepted: August 26, 2008

DOI: 10.1007/s10973-008-9045-8